Research Article

Parametric Controller Design of Hopf Bifurcation System

Jinbo Lu, Xiaorong Hou, and Min Luo

School of Energy Science and Engineering, University of Electronic Science and Technology of China, Chengdu, Sichuan 611131, China

Correspondence should be addressed to Xiaorong Hou; houxr@uestc.edu.cn

A general parametric controller design method is proposed for Hopf bifurcation of nonlinear dynamic system. This method does not increase the dimension of the system. Compared with the existing methods, the controller designed by this method has a lower controller order and a simpler structure, and it does not contain equilibrium points. The method keeps equilibrium of the origin system unchanged. Symbolic computation is used to deduce the constraints of controller, and cylindrical algebraic decomposition is used to find the stability parameter regions in parameter space of controller. The method is then employed for Hopf bifurcation control. Taking Lorenz system as an example, the controller design steps of the method and numerical simulations are discussed. Computer simulation results are presented to confirm the analytical predictions.

1. Introduction

Bifurcation is a normal phenomenon of nonlinear system, and the research in bifurcation control has achieved considerable progress in the past 30 years [1]. Hopf bifurcation is an important type of bifurcation. Its practical significance lies in the notion that Hopf bifurcation is a critical state between stable and unstable. There are a lot of related research achievements [2–4], covering a lot of fields, including power system [5, 6], electronic technology [7], network technology [8], new energy [9], and optical technology [10].

Hopf bifurcation research focused on phenomena analysis [11–13] and bifurcation control [14–19]. And the work of Hopf bifurcation control is designing control strategy for Hopf bifurcation system to modify the original system dynamic characteristics [16, 18, 20]. But the general applications of these designed controls are still limited. For enhancing flexibility and universality of Hopf bifurcation controller, some study of applying parametric control to Hopf bifurcation system controller design has emerged [17, 21].

On the basis of nonlinear state feedback theory, [17] gives a relatively common form of Hopf bifurcation control,

complete solution, and simulation of controller parameters by example. Its controller is

$$
\begin{aligned}
u_q &\left(X, X_1^*, X_2^*, \ldots, X_k^*, \mu \right) \\
&= \sum_{i=1}^{n} A_{qi} \prod_{j=1}^{k} \left(x_i - x_{ij}^* \right) \\
&\quad + \sum_{i=1}^{n} \sum_{j=1}^{k} B_{qij} \left(x_i - x_{ij}^* \right) \prod_{p=1}^{k} \left(x_i - x_{ip}^* \right) \\
&\quad + \sum_{i=1}^{n} \sum_{j=1}^{k} C_{qij} \left(x_i - x_{ij}^* \right)^2 \prod_{p=1}^{k} \left(x_i - x_{ip}^* \right) \\
&\quad + \sum_{i=1}^{n} \sum_{j=1}^{k} D_{qij} \left(x_i - x_{ij}^* \right)^2 \prod_{p=1}^{k} \left(x_i - x_{ip}^* \right)^2 + \cdots \\
&\qquad\qquad\qquad\qquad\qquad (q = 1, 2, \ldots, n),
\end{aligned}
$$

$$(1)$$

where X is system state vector, $X_1^*, X_2^*, \ldots, X_k^*$ are k equilibrium points of system, A_{qi}, B_{qij}, C_{qij}, and D_{qij} are the controller parameters, x_i is i state of system, and x_{ij}^* and

x_{ip}^* are j and p equilibrium point value of system state x_i, respectively.

As can be seen from controller expression, the controller in [17] contains all of the system equilibrium points. The paper [21] has done a further study on the basis of [17]. The parameters of the controller have been simplified significantly, for a 3-dimensional system with two equilibrium points (the Rössler system). The controller in [21] is

$$u_3 = \sum_{i=1}^{3} \Big[A_i \left(x_i - x_{i0}^+ \right) \left(x_i - x_{i0}^- \right)$$
$$+ B_i \left(x_i - x_{i0}^+ \right)^2 \left(x_i - x_{i0}^- \right) \qquad (2)$$
$$+ B_{i+3} \left(x_i - x_{i0}^+ \right) \left(x_i - x_{i0}^- \right)^2 \Big],$$

where A_i, B_i, and B_{i+3} are the system parameters and x_{i0}^+ and x_{i0}^- are the value of system state x_i on the two equilibrium points. In addition to the controller design work, [21] used plane figure to display the controller constraints and analyzed the bifurcation cases of each connected region.

Although the deep research of Hopf bifurcation control has been done in [17, 21], there are still some limitations. For example, the controller has a complicated form and higher order and includes system equilibrium points, and its parameters constraint solution is cumbersome. Besides, in [17], solution of controller parameters is not sufficient and intuitive. It just expresses several groups of controller parameters by inequality form. Except for the study of [17, 21], [22] did a further application in parametric method on the basis of [21].

In view of the above questions, in this paper, the controller form is improved, and a simple and general parametric controller design method is presented. The designed controller has lower order, and there is no inclusion of system equilibrium points.

The remainder structure of this paper is as follows. Section 2 provides description of Hopf bifurcation system and the method and procedure of parametric controller design. Lorenz system is taken as an example in Section 3; this section designs the related parametric controller and deduces the constraints. In Section 4, numerical simulations are calculated. And in Section 5, the conclusion of this paper is given.

2. A Hopf Bifurcation System Description and Parametric Controller Design

2.1. Hopf Bifurcation System Description. Before discussing how to design a controller for Hopf bifurcation, a general formula of the Hopf bifurcation system is presented. To be more specific, consider the following general nonlinear system:

$$\dot{X} = F\left(X, \mu \right) = \left[f_1 \left(X, \mu \right), f_2 \left(X, \mu \right), \dots, f_n \left(X, \mu \right) \right]^T, \quad (3)$$

where the dot denotes differentiation with respect to time t and $X = \left(x_1, x_2, \dots, x_n \right)^T \in R^n$ is an n-dimensional

state vector, while $\mu \in R$ is a scalar parameter, called bifurcation parameter (note: it can be assumed that μ is an m-dimensional vector for $m \geq 1$). $F(X, \mu)$ is a matrix of nonlinear polynomial system with Hopf bifurcations, and the following conditions must be satisfied:

(1) Let X^* be an equilibrium (or fixed point) of the system; that is, $F(X^*, \mu) \equiv 0$, for any value of μ.

(2) Suppose that the Jacobian of the system evaluated at the equilibrium X^* has eigenvalues, $\lambda_j(\mu)$, $j = 1, 2, \dots, n$, which may be real or complex. Assume there exists one pair of the complex conjugates $\lambda_1(\mu)$, $\lambda_2(\mu)$, and all of the others are in left half of complex plane.

(3) Suppose that $\lambda_{1,2}(\mu) = \alpha(\mu) \pm i\beta(\mu)$ cross the imaginary axis at $\mu = \mu^*$. When $\mu = \mu^*$, $\alpha(\mu^*) = 0$, $d\alpha(\mu^*)/dt \neq 0$, and $\beta(\mu^*) \neq 0$. According to the Hopf theory, a family of limit cycles will bifurcate from the equilibrium X^* at the critical point μ^*.

2.2. Generic Parametric Controller Description. For system (3), we design a general formula of nonlinear state feedback control:

$$\dot{X} = F\left(X, \mu \right) + u\left(X, \mu \right), \qquad (4)$$

where

$$u\left(X, \mu \right) = \left[0, 0, \dots, u_j \left(X, \mu \right), 0, \dots, 0 \right]^T,$$
$$u_j = g\left(X, \mu \right) f_j \left(X, \mu \right) + \sum_{i=1, i \neq j}^{n} c_{0i} f_i \left(X, \mu \right); \qquad (5)$$

here,

$$g\left(X, \mu \right) = c_1 + \sum_{k=1}^{n} \left(c_{k+1} x_k + c_{n+k+1} x_k^2 \right), \qquad (6)$$

and $\{ c_{0i}, c_1, c_{k+1}, c_{n+k+1} \in R \}$ are the parameters of controller. In the controller, the form of $g(X, \mu)$ is simple. $g(X, \mu)$ is the polynomial of system states and it is not including system equilibrium point (generally, the quadratic term is not needed). Comparing with [17], the designed controller is simpler and has lower order and is not including system equilibrium point. Under the control u, in order to keep all the original equilibria unchanged for controlled system (4), the following conditions must be satisfied:

$$u\left(X^*, \mu \right) = 0,$$
$$u\left(X, \mu^* \right) \neq 0. \qquad (7)$$

Remark 1. The control equation given in (5) is not a unique control law. There are many other feasible controllers that may satisfy the system. In (5), the controller consists of system polynomial; $c_{0i} \in R$ also can change for $c_{0i} \in R^n$. That is to say, c_{0i} can be a one-dimensional parameter, which also can be a polynomial composed of system states. So on the premise of satisfying system requests, c_{0i} has a variety of possible

expressions, covered by all linear combinations composed of system states, and then it includes the controller expression proposed by [17].

Remark 2. There may not be only one component in $u(X, \mu)$, but usually one component can satisfy the control system requests, so we only design one component here. Besides, as you can see, no matter how many components it has, there will be no inclusion of system equilibrium points value in controller $u(X, \mu)$.

Remark 3. $g(X, \mu)$ form is not fixed. Higher polynomial can be introduced in it. Here, in order to reduce the controller order, $g(X, \mu)$, the highest order is 2, and in most cases, 1 order $g(X, \mu)$ is enough.

2.3. Parametric Controller Design Steps. For explaining parametric controller design method and steps, a 3-dimension system controller is designed as an example in this paper. The controller design steps are as follows.

Step 1. According to the parametric controller equation, a 3-dimension system with Hopf bifurcation is given:

$$
\begin{aligned}
\dot{x}_1 &= f_1(X, \mu), \\
\dot{x}_2 &= f_2(X, \mu), \\
\dot{x}_3 &= f_3(X, \mu).
\end{aligned} \tag{8}
$$

Here, $X = [x_1, x_2, x_3]^T$. Then, system (8) has parametric controller:

$$
u(X, \mu) = [u_1(X, \mu), u_2(X, \mu), u_3(X, \mu)]^T, \tag{9}
$$

$$
u_j(X, \mu) = g(X, \mu) f_j(X, \mu) + \sum_{k=1}^{n} c_{0k} f_k(X, \mu); \tag{10}
$$

here, $\{u_j(X, \mu) \neq 0, u_k(X, \mu) = 0, k \neq j, j = 1, 2, 3\}$, $g(X) = c_1 + c_2 x_1 + c_3 x_2 + c_4 x_3$, $\{c_{0k}, c_i \in R, i = 1, 2, 3, 4\}$, and c_{0k} and c_i are controller parameters.

In order to make concise expression, without loss of generality, controller (10) can be written as simplifying form:

$$
u_2(X, \mu) = g(X, \mu) \cdot f_2(X, \mu) + c_{01} f_1(X, \mu). \tag{11}
$$

Step 2. According to the closed-loop system expression after adding controller, we can get Jacobian matrix including controller parameters. Adding controller (11) on system (8), closed-loop expression can be written as

$$
\begin{aligned}
\dot{x}_1 &= f_1(X, \mu), \\
\dot{x}_2 &= f_2(X, \mu) + u_2(X, \mu), \\
\dot{x}_3 &= f_3(X, \mu).
\end{aligned} \tag{12}
$$

At this point, the Jacobian matrix of closed-loop system can be described as

$$
J = \begin{bmatrix} \dfrac{\partial f_1}{\partial x_1} & \dfrac{\partial f_1}{\partial x_2} & \dfrac{\partial f_1}{\partial x_3} \\[2mm] j_{21} & j_{22} & j_{23} \\[2mm] \dfrac{\partial f_3}{\partial x_1} & \dfrac{\partial f_3}{\partial x_2} & \dfrac{\partial f_3}{\partial x_3} \end{bmatrix}, \tag{13}
$$

where

$$
\begin{aligned}
j_{21} &= \frac{\partial f_2}{\partial x_1} + \frac{\partial f_2}{\partial x_1} g(X) + c_2 f_2 + c_{01} \frac{\partial f_1}{\partial x_1}, \\
j_{22} &= \frac{\partial f_2}{\partial x_2} + \frac{\partial f_2}{\partial x_2} g(X) + c_3 f_2 + c_{01} \frac{\partial f_1}{\partial x_2}, \\
j_{23} &= \frac{\partial f_2}{\partial x_3} + \frac{\partial f_2}{\partial x_3} g(X) + c_4 f_2 + c_{01} \frac{\partial f_1}{\partial x_3}.
\end{aligned} \tag{14}
$$

Step 3. In accordance with the gotten Jacobian matrix, we can compute system characteristic equation at the system equilibrium point. Supposing one equilibrium point of system (8) is X_0, then according to the Jacobian matrix, the characteristic equation at the system equilibrium point can be described as follows:

$$
D(\lambda) = \det(\lambda I - J)|_{X=X_0} = a_0 \lambda^3 + a_1 \lambda^2 + a_2 \lambda + a_3; \tag{15}
$$

here,

$$
a_0 = 1,
$$

$$
a_1 = \left[-c_{01} \frac{\partial f_1}{\partial x_2} - \frac{\partial f_1}{\partial x_1} - \frac{\partial f_2}{\partial x_2} g(X) - \frac{\partial f_3}{\partial x_3} \right. \\ \left. - c_3 f_2 \right]_{X=X_0},
$$

$$
a_2 = \left[\left(\frac{\partial f_1}{\partial x_1} \frac{\partial f_2}{\partial x_2} - \frac{\partial f_1}{\partial x_2} \frac{\partial f_2}{\partial x_1} - \frac{\partial f_2}{\partial x_3} \frac{\partial f_3}{\partial x_2} + \frac{\partial f_2}{\partial x_2} \frac{\partial f_3}{\partial x_3} \right) \right. \\
\cdot g(X) - c_2 \frac{\partial f_1}{\partial x_2} f_2 - c_4 \frac{\partial f_3}{\partial x_2} f_2 + c_3 f_2 \left(\frac{\partial f_3}{\partial x_3} + \frac{\partial f_1}{\partial x_1} \right) \\
+ c_{01} \left(\frac{\partial f_3}{\partial x_3} \frac{\partial f_1}{\partial x_2} - \frac{\partial f_1}{\partial x_3} \frac{\partial f_3}{\partial x_2} \right) + \frac{\partial f_1}{\partial x_1} \frac{\partial f_2}{\partial x_2} + \frac{\partial f_1}{\partial x_1} \frac{\partial f_3}{\partial x_3} \\
\left. - \frac{\partial f_1}{\partial x_2} \frac{\partial f_2}{\partial x_1} - \frac{\partial f_1}{\partial x_3} \frac{\partial f_3}{\partial x_1} - \frac{\partial f_2}{\partial x_3} \frac{\partial f_3}{\partial x_2} + \frac{\partial f_2}{\partial x_2} \frac{\partial f_3}{\partial x_3} \right]_{X=X_0},
$$

$$
a_3 = \left[\left(-\frac{\partial f_1}{\partial x_1} \frac{\partial f_2}{\partial x_2} \frac{\partial f_3}{\partial x_3} + \frac{\partial f_1}{\partial x_1} \frac{\partial f_2}{\partial x_3} \frac{\partial f_3}{\partial x_2} + \frac{\partial f_1}{\partial x_2} \frac{\partial f_2}{\partial x_1} \frac{\partial f_3}{\partial x_3} \right. \right. \\
\left. - \frac{\partial f_1}{\partial x_2} \frac{\partial f_2}{\partial x_3} \frac{\partial f_3}{\partial x_1} - \frac{\partial f_1}{\partial x_3} \frac{\partial f_2}{\partial x_1} \frac{\partial f_3}{\partial x_2} + \frac{\partial f_1}{\partial x_3} \frac{\partial f_2}{\partial x_2} \frac{\partial f_3}{\partial x_1} \right) \\
\cdot g(X) + \left(-c_3 \frac{\partial f_1}{\partial x_1} \frac{\partial f_3}{\partial x_3} + c_4 \frac{\partial f_1}{\partial x_1} \frac{\partial f_3}{\partial x_2} - c_4 \frac{\partial f_1}{\partial x_2} \frac{\partial f_3}{\partial x_1} \right.
$$

$$
\begin{aligned}
&+ c_2 \frac{\partial f_1}{\partial x_2} \frac{\partial f_3}{\partial x_3} + c_3 \frac{\partial f_1}{\partial x_3} \frac{\partial f_3}{\partial x_1} - c_2 \frac{\partial f_1}{\partial x_3} \frac{\partial f_3}{\partial x_2} \Bigg) f_2 - \frac{\partial f_1}{\partial x_1} \\
&\cdot \frac{\partial f_2}{\partial x_2} \frac{\partial f_3}{\partial x_3} + \frac{\partial f_1}{\partial x_1} \frac{\partial f_2}{\partial x_3} \frac{\partial f_3}{\partial x_2} + \frac{\partial f_1}{\partial x_2} \frac{\partial f_2}{\partial x_1} \frac{\partial f_3}{\partial x_3} - \frac{\partial f_1}{\partial x_2} \\
&\cdot \frac{\partial f_2}{\partial x_3} \frac{\partial f_3}{\partial x_1} - \frac{\partial f_1}{\partial x_3} \frac{\partial f_2}{\partial x_1} \frac{\partial f_3}{\partial x_2} + \frac{\partial f_1}{\partial x_3} \frac{\partial f_2}{\partial x_2} \frac{\partial f_3}{\partial x_1} \Bigg]_{X=X_0} .
\end{aligned}
\tag{16}
$$

Remark 4. X_0 does not require the actual solution. It is only a formal symbol. You can see the specific condition in the subsequent computation example; X_0 in Step 4 is the same as here.

Step 4. Using Hurwitz criterion, we can get the stable constraint of system and simplify it by polynomial division. According to Hurwitz criterion, the constraints including controller parameter are

$$
\begin{aligned}
&a_0 > 0, \\
&a_1 > 0, \\
&a_2 > 0, \\
&a_3 > 0, \\
&g = a_1 a_2 - a_0 a_3 \geq 0.
\end{aligned}
\tag{17}
$$

Considering $a_0 = 1$, the system stable constraints can be written as

$$
\begin{aligned}
&a_1 > 0, \\
&a_2 > 0, \\
&a_3 > 0, \\
&g = a_1 a_2 - a_3 \geq 0.
\end{aligned}
\tag{18}
$$

In accordance with polynomial division, for k order real polynomial $B(X)$ and m order real polynomial $A(X)$, $X \in R^n$, $k \geq 1, m \geq 1$, $A(X)$ can be written as

$$
A(X) = \overline{A}(X) B(X) + L_{A/B}(X);
\tag{19}
$$

here, $\overline{A}(X)$ is the integral part of $A(X)$ divided by $B(X)$ and $L_{A/B}(X)$ is the residue of $A(X)$ divided by $B(X)$. If $B(X_0) = 0$ at X_0, then $L_{A/B}(X_0) = A(X_0)$. Supposing $G(X) = 0$ is system (8) equilibrium point equation and X_0 is the equilibrium, then the system constraints can be simplified as

$$
S : \begin{cases}
l_1 = L_{a_1/G}(X_0) > 0 \\
l_2 = L_{a_2/G}(X_0) > 0 \\
l_3 = L_{a_3/G}(X_0) > 0 \\
l_4 = L_{g/G}(X_0) > 0.
\end{cases}
\tag{20}
$$

Step 5. Using computer algebra tools such as symbol computation software and cylindrical algebraic decomposition algorithm to solve semialgebraic set composed of (20) and equilibrium point equation $G(X) = 0$, we can get controller parameter space satisfying system requests.

Remark 5. In constraints l_4, when $l_4 = 0$, Hopf bifurcation occurs, at which the system is critically stable, and its state characteristic is continuous oscillation. If $l_4 > 0$, the system is stable and the state is convergent.

3. Lorenz System Controller Design

It is well known that the Lorenz system widely exists in various research areas [23–26] and it can exhibit complex dynamics, including equilibria, limit cycles, and chaos. This section will explain the controller design and verification process by Lorenz system.

3.1. Lorenz System Description. According to [17], Lorenz system can be described as

$$
\begin{aligned}
\dot{x} &= -a(x - y), \\
\dot{y} &= bx - xz - y, \\
\dot{z} &= xy - cz,
\end{aligned}
\tag{21}
$$

in which a, b, and c are variable parameters. These parameters have direct effect on system characteristics. A little change of them may change the system state and make system trajectory turn from stable to bifurcation and even chaos [17]. According to (21), we can obtain system equilibrium point equation:

$$
x_0^3 - (bc - c) x_0 = 0.
\tag{22}
$$

3.2. Controller Design. In accordance with (11), controller can be designed as

$$
u_2 = \dot{y} (c_1 + c_2 x + c_3 y + c_4 z) + c_0 \dot{x},
\tag{23}
$$

where $c_0 \in R, c_1 \in R, c_2 \in R, c_3 \in R$, and $c_4 \in R$ are controller parameters. According to (21), controller can be rewritten as

$$
\begin{aligned}
u_2 = {}& (bx - xz - y)(c_1 + c_2 x + c_3 y + c_4 z) \\
& - c_0 a(x - y).
\end{aligned}
\tag{24}
$$

Compared with the existing research work [17, 21], (24) has a more concise expression, and it does not include equilibrium point value.

3.3. System Stable and Hopf Bifurcation Condition Computation. Lorenz system state characteristics will be directly affected by system parameters. In order to verify controller performance, we select system parameters $a = 4, b = 16$, and $c = 1$. When there is no controller, system state trajectory is chaotic. Taking system parameters in Lorenz system (21), we can obtain a new system:

$$
\begin{aligned}
\dot{x} &= -4(x - y), \\
\dot{y} &= 16x - xz - y, \\
\dot{z} &= xy - z.
\end{aligned}
\tag{25}
$$

In accordance with (25), the equation at system equilibrium point is

$$x_0^3 - 15x_0 = 0. \tag{26}$$

For simplifying computation process, let $c_0 = 0$, $c_3 = 0$, and the controller can be simplified as

$$u_2(x, y, z) = \dot{y}(c_1 + c_2 x + c_4 z). \tag{27}$$

Taking in (27), after computation and arrangement, we can get system constraints:

$$l_1 = c_4 x_0^2 + c_2 x_0 + c_1 + 6, \tag{28}$$

$$l_2 = (5 + 5c_1 + 16c_4) x_0^2 + 16c_2 x_0 - 59c_1 - 55, \tag{29}$$

$$l_3 = (120c_4 + 12c_1 + 12) x_0^2 + 120c_2 x_0 - 60c_1 - 60, \tag{30}$$

$$l_4$$
$$= \left(5c_1^2 + 16c_2^2 + 240c_4^2 + 32c_1 c_4 + 23c_1 - 4c_4 + 18\right) x_0^2$$
$$+ \left(32c_1 c_2 + 480c_2 c_4 - 4c_2\right) x_0 - 59c_1^2 - 349c_1$$
$$- 270. \tag{31}$$

Combined with (26) at equilibrium point, constraints equations (28)~(31) constitute a semialgebra set. Using computer algebra tools, we can simplify the semialgebra set. The arranged system constraints are as follows:

$$-5 \le c_1 < -1,$$
$$c_1 + 15c_4 + 1 > 0,$$
$$-15c_2^2 + (c_1 + 15c_4 + 1)^2 > 0, \tag{32}$$
$$15c_2^2 + \left(c_1 + 15c_4 - \frac{1}{8}\right)^2 - \frac{1}{64} > 0,$$
$$\varphi \ge 0,$$

where

$$\varphi = \left(c_1^2 - 15c_2^2 + 255c_4^2 + 30c_1 c_4\right)\left(16c_1^2 - 240c_2^2 + 3600c_4^2 + 480c_1 c_4 - 120c_4 - 8c_1 + 1\right). \tag{33}$$

In (32), if $c_1 = -5$ or $\varphi = 0$, the Hopf bifurcation will happen in system. The constraints listed in (32) can use cylindrical algebraic decomposition algorithm to calculate the controller parameter space. But the 3-dimension decomposition result is still not intuitive. In the following numerical simulation, we will assign a certain value to c_1 and then mark out the controller parameter range in 2-dimension space.

4. Simulations

4.1. Constraints Calculation. Through the above analysis results, we can see $c_1 \in [-5, -1)$. If the system is required to be stable, parameter c_1 should satisfy $c_1 \in (-5, -1)$. Because
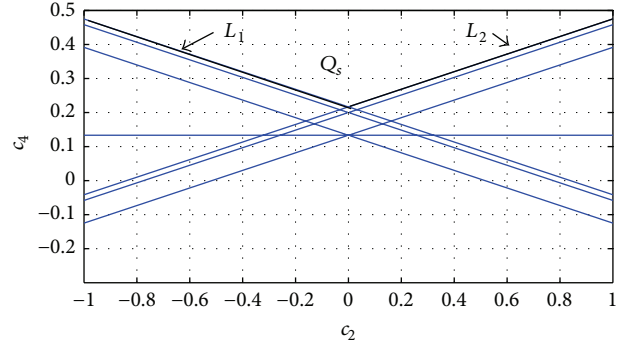

FIGURE 1: System constraints curves in c_2-c_4 plane when $c_0 = 0$ and $c_1 = -3$.

the system has a bifurcation when $c_1 = -5$, we can choose two different conditions $c_1 = -3$ and $c_1 = -5$ for analysis in numerical simulation.

When $c_1 = -3$, Lorenz system constraints (32) can be rewritten as

$$c_4 > \frac{2}{15},$$
$$-15c_2^2 + 225c_4^2 - 60c_4 + 4 > 0,$$
$$15c_2^2 + 225c_4^2 - \frac{375}{4}c_4 + \frac{39}{4} > 0, \tag{34}$$
$$\varphi = \left(5c_2^2 - 75c_4^2 + 30c_4 - 3\right)$$
$$\cdot \left(240c_2^2 - 3600c_4^2 + 1560c_4 - 169\right) \ge 0.$$

When $c_1 = -5$, system constraints (32) can be rewritten as

$$c_4 > \frac{4}{15},$$
$$-15c_2^2 + 225c_4^2 - 120c_4 + 16 > 0,$$
$$15c_2^2 + 225c_4^2 - \frac{615}{4}c_4 + \frac{105}{4} > 0, \tag{35}$$
$$\varphi = \left(-3c_2^2 + 45c_4^2 - 30c_4 + 5\right)$$
$$\cdot \left(-80c_2^2 + 1200c_4^2 - 840c_4 + 147\right) \ge 0.$$

4.2. Controller Parameter Region. As shown in Figure 1, implicit function curves of constraints (34) equations are drawn in the 2-dimension space. According to cylindrical algebraic decomposition algorithm, we can search the space divided by these function curves; then region Q_s is found. In the region, c_2 and c_4 can stabilize system. The boundary curves of Q_s are L_1 and L_2, and L_1 and L_2 are part of $\varphi = 0$ in (34). L_1 is line $60c_2 + 60\sqrt{15}c_4 - 13\sqrt{15} = 0$ when $c_2 \le 0$; L_2 is line $-60c_2 + 60\sqrt{15}c_4 - 13\sqrt{15} = 0$ when $c_2 \ge 0$.

In order to provide a convenient explanation, we suppose the three equilibrium points of (26) are E_0, E_-, and E_+, where E_- and E_+ are a pair of symmetric equilibrium points. For
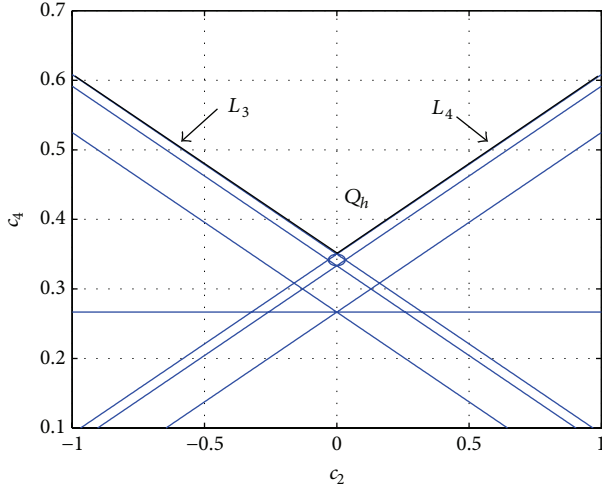
FIGURE 2: System constraints curves in c_2-c_4 plane when $c_0 = 0$ and $c_1 = -5$.
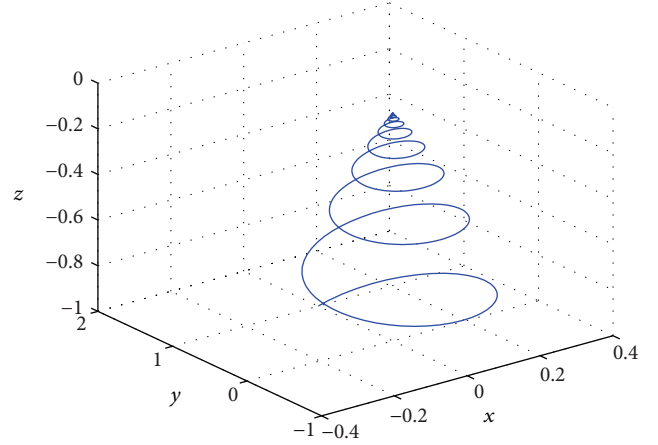

FIGURE 3: The Lorenz system trajectory is stable at E_0 when $c_1 = -3$.

parameter space solved by constraints (34), the system state at E_0 is convergent. Choosing different parameters can decide whether there is a bifurcation at system equilibrium points E_- and E_+: (i) there is no existing Hopf bifurcation at two equilibrium points, while the system states are stable, and at the moment the controller parameters c_2 and c_4 value should be in Q_s but not on the boundary; (ii) system states are stable at equilibrium point E_- while at E_+ there is a Hopf bifurcation, and at the moment controller parameter value should on the boundary L_1; (iii) there is a Hopf bifurcation at equilibrium point E_- while system is stable at E_+, and at the moment controller parameter should be on the boundary L_2; (iv) there are Hopf bifurcations at both equilibrium points, and at the moment controller parameter should be on the cross point of L_1 and L_2.

The implicit function curves of constraints (35) equations are shown in Figure 2. Similar to constraints (34), using cylindrical algebraic decomposition algorithm, we can find the parameter space Q_h which satisfies the control requirements. The boundaries of region Q_h are lines L_3 and L_4. They are part of $\varphi = 0$ in (35). L_3 is line $20c_2 + 20\sqrt{15}c_4 - 7\sqrt{15} = 0$ when $c_2 \leq 0$, and L_4 is line $-20c_2 + 20\sqrt{15}c_4 - 7\sqrt{15} = 0$ when $c_2 \geq 0$.

Unlike constraints (34), there is a Hopf bifurcation at E_0 in (26) by this time. According to the different states at equilibrium points E_- and E_+, the cases are as follows: (i) both equilibria become stable without Hopf bifurcations; at the moment, the controller parameters c_2 and c_4 value should be selected in Q_h and should not be on the boundary; (ii) the system states are stable at equilibrium point E_-, while there is a Hopf bifurcation at E_+, and at the moment controller parameter value should on the boundary L_3; (iii) there is a Hopf bifurcation at equilibrium point E_-, while at E_+, system is stable, and at the moment controller parameter should be on the boundary L_4; (iv) there are Hopf bifurcations at both equilibrium points, and at the moment controller parameter should be on the cross point of L_3 and L_4.

FIGURE 4: Stable trajectory at E_-, when $c_1 = -3$, for case (i).
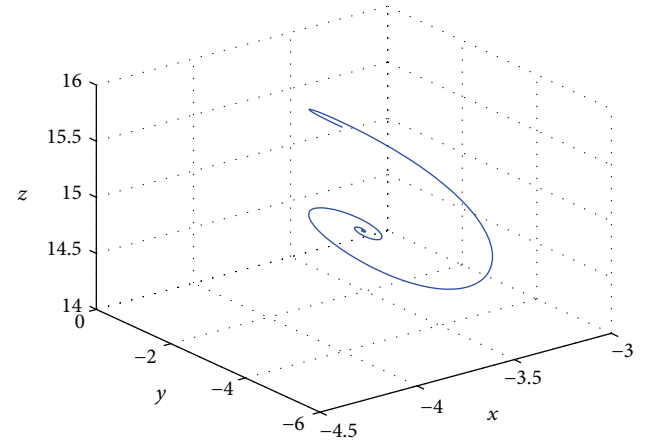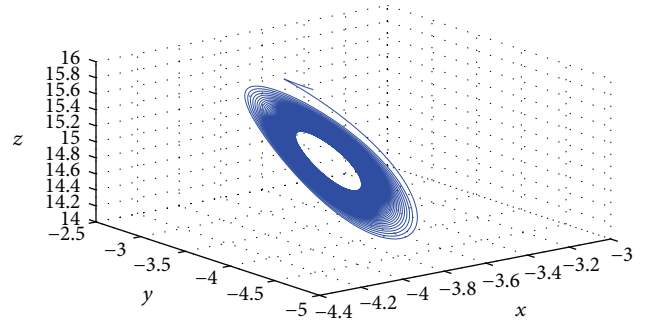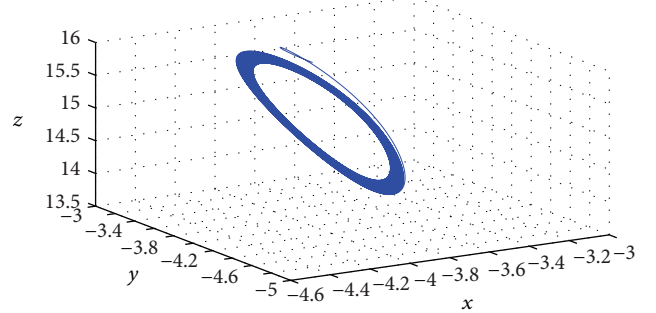
4.3. Numeric Simulation Computation Near Equilibria.
According to the different conditions at three equilibrium points, we compute the controller parameters below. In order to explain the validity of solved controller parameter range, we conduct the numeric simulation of state stability near equilibrium points for Lorenz system (25). The simulation results are shown in Figures 3–20. When simulating, the initial values of system equilibrium points E_0, E_-, and E_+ are $(0, 1, -1)$, $(-4, -4, 16)$, and $(4, 4, 16)$.

When controller parameter $c_1 = -3$, the system trajectory at E_0 is convergent, while according to the different cases of E_- and E_+, parameters c_2 and c_4 can be selected as follows: (i) when the system is stable at two equilibrium points, we can select $c_2 = 1$, $c_4 = 1$; (ii) system is stable at equilibrium point E_-, while at E_+ it has a Hopf bifurcation, and at the moment we can select $c_2 = -1$, $c_4 = (1/60)(13 + 4\sqrt{15}) \approx 0.47487$; (iii) there is a Hopf bifurcation at equilibrium point E_-, while system is stable at E_+, and at the moment we can select $c_2 = 1$, $c_4 = (1/60)(13 + 4\sqrt{15}) \approx 0.47487$; (iv) both equilibria E_- and E_+ have Hopf bifurcations, and at the moment we can select $c_2 = 0$, $c_4 = 13/60 \approx 0.21667$.
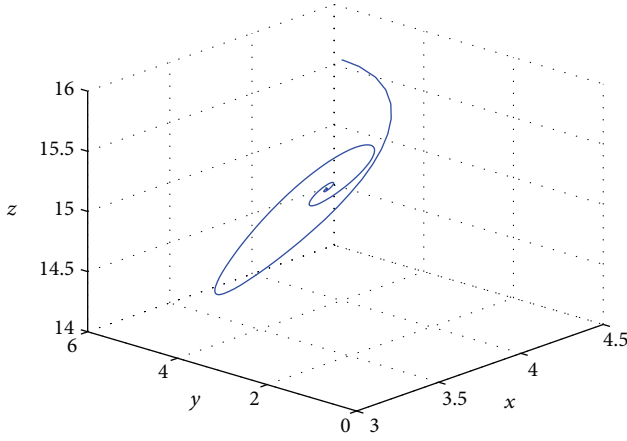
FIGURE 5: Stable trajectory at E_+, when $c_1 = -3$, for case (i).
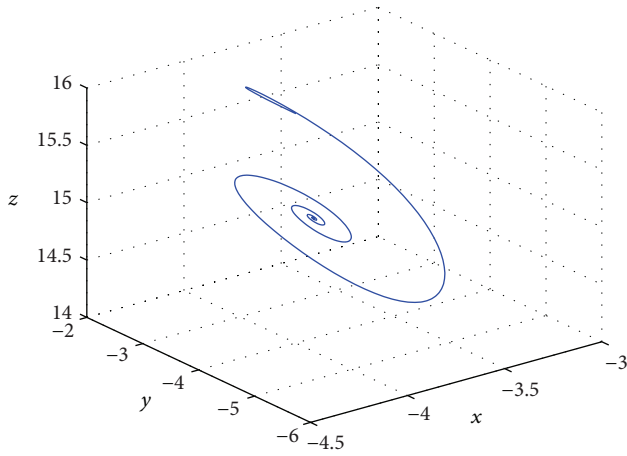
FIGURE 6: Stable trajectory at E_-, when $c_1 = -3$, for case (ii).
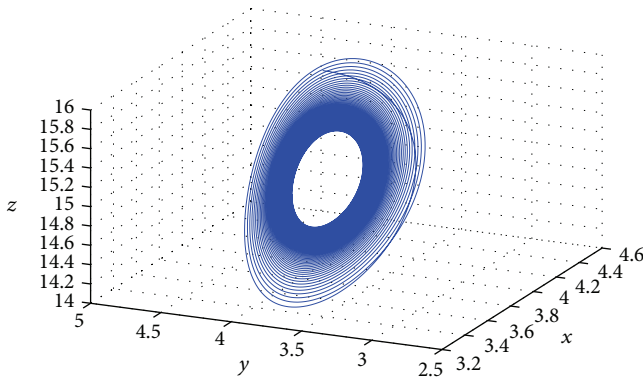
FIGURE 7: Hopf bifurcation at E_+, when $c_1 = -3$, for case (ii).

FIGURE 8: Hopf bifurcation at E_-, when $c_1 = -3$, for case (iii).
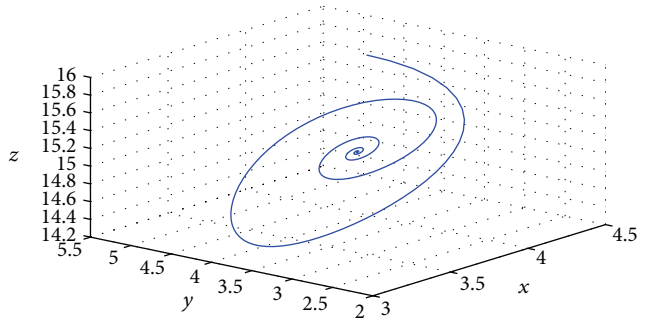
FIGURE 9: Stable trajectory at E_+, when $c_1 = -3$, for case (iii).

FIGURE 10: Hopf bifurcation at E_-, when $c_1 = -3$, for case (iv).

In Figure 3 the Lorenz system trajectory is convergent at E_0 when $c_1 = -3$. Figures 4–11 are system simulation trajectories for different cases of E_- and E_+, in which, corresponding to case (i), Figure 4 is the stable convergent trajectory at E_-, and Figure 5 is the stable convergent trajectory at E_+. Corresponding to case (ii), Figure 6 is the stable convergent trajectory at E_-, and Figure 7 is the system trajectory of Hopf bifurcation at E_+. For case (iii), Figure 8 is the Hopf bifurcation trajectory at E_-, and Figure 9 is the stable convergent trajectory at E_+. Figures 10 and 11 are the system trajectories of Hopf bifurcation at E_- and E_+ for case (iv).

When controller parameter $c_1 = -5$, system has Hopf bifurcation at E_0, and its trajectory is a limit cycle. And according to different cases at E_- and E_+, parameters c_2 and c_4 can be chosen as follows: (i) when the system is stable at two equilibrium points, we can select $c_2 = 1$, $c_4 = 1$; (ii) system is stable at equilibrium point E_-, while there is a Hopf bifurcation at E_+, and at the moment we can select $c_2 = -1$, $c_4 = (1/60)(21 + 4\sqrt{15}) \approx 0.60819$; (iii) there is a Hopf bifurcation at equilibrium point E_-, while system is stable at E_+, and at the moment we can select $c_2 = 1$, $c_4 = (1/60)(21 + 4\sqrt{15}) \approx 0.60819$; (iv) there are Hopf bifurcations at both equilibria, and we can select $c_2 = 0$, $c_4 = 7/20 = 0.35$.
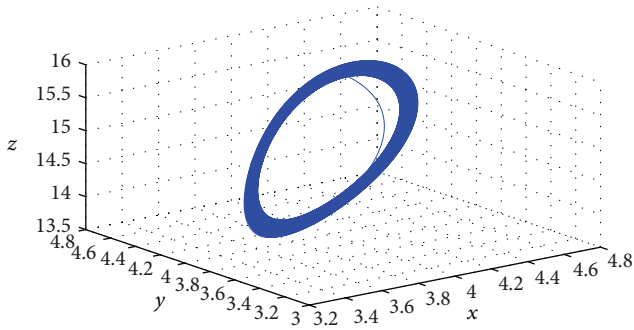
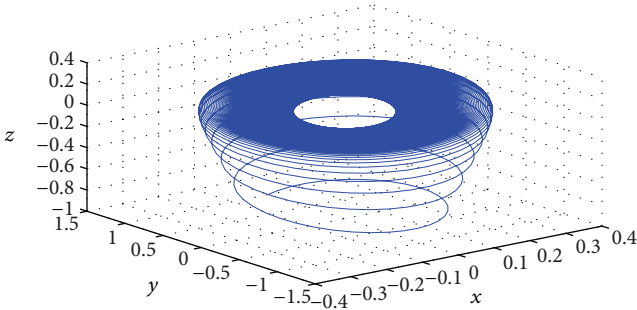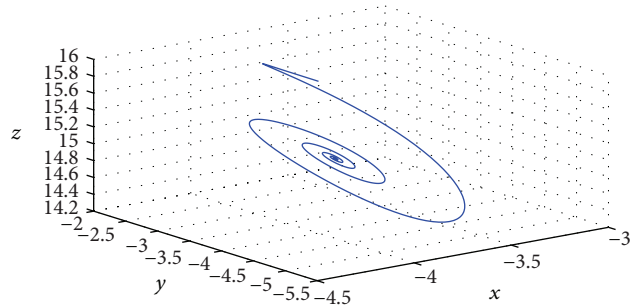FIGURE 11: Hopf bifurcation at E_+, when $c_1 = -3$, for case (iv).
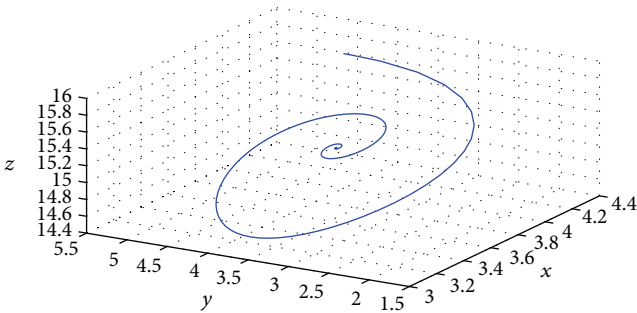

FIGURE 15: Stable trajectory at E_-, when $c_1 = -5$, for case (ii).

FIGURE 12: System Hopf bifurcation trajectory at E_0 when $c_1 = -5$.

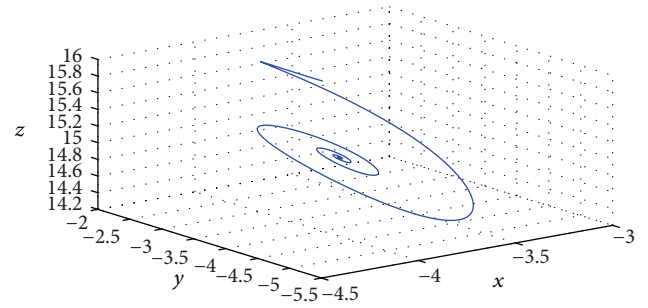FIGURE 16: Hopf bifurcation at E_+, when $c_1 = -5$, for case (ii).

FIGURE 13: Stable trajectory at E_-, when $c_1 = -5$, for case (i).

FIGURE 17: Hopf bifurcation at E_-, when $c_1 = -5$, for case (iii).

FIGURE 14: Stable trajectory at E_+, when $c_1 = -5$, for case (i).

FIGURE 18: Stable trajectory at E_+, when $c_1 = -5$, for case (iii).

Figure 12 is the system Hopf bifurcation trajectory at E_0 when $c_1 = -5$, and at this moment system converges to a stable limit cycle. Figures 13–20 are system simulation trajectories at E_- and E_+ for different cases, in which,

according to case (i), Figures 13 and 14 are the stable trajectories at E_- and E_+. In accordance with case (ii), Figure 15
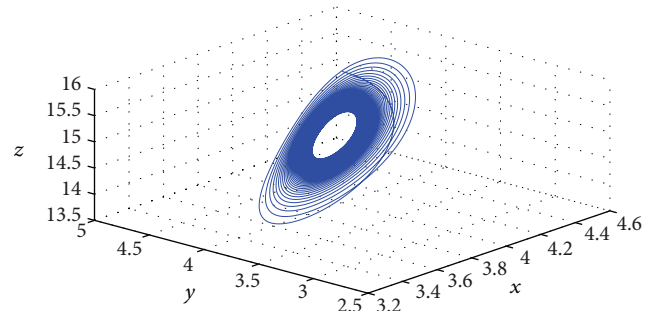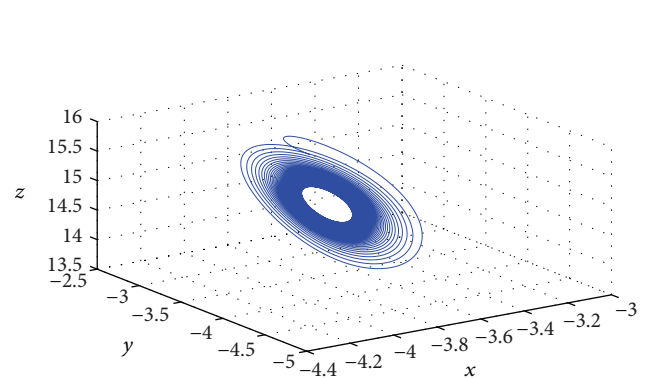
FIGURE 19: Hopf bifurcation at E_-, when $c_1 = -5$, for case (iv).

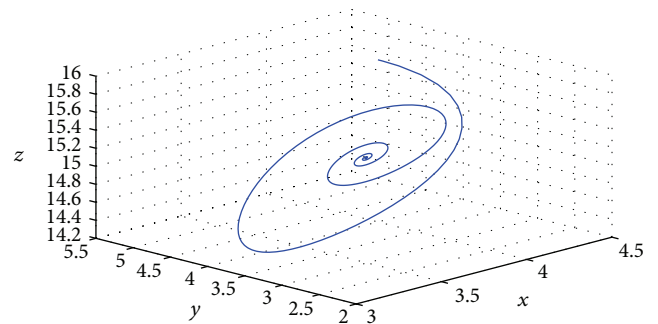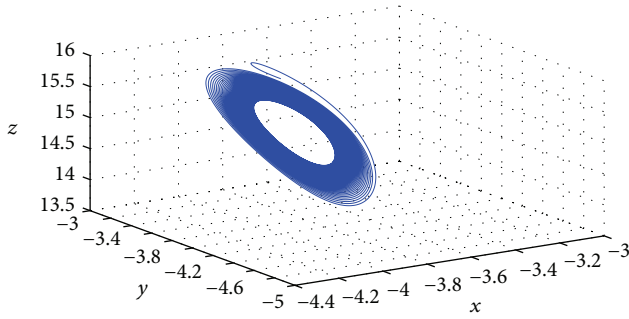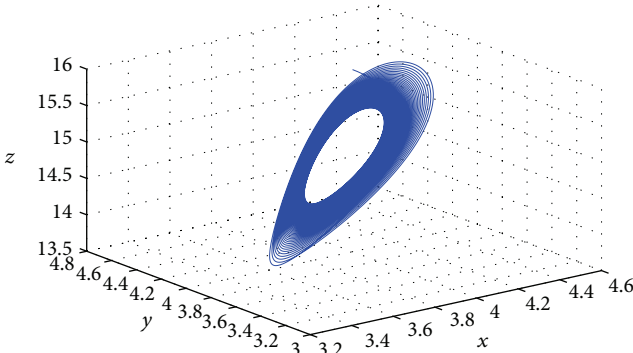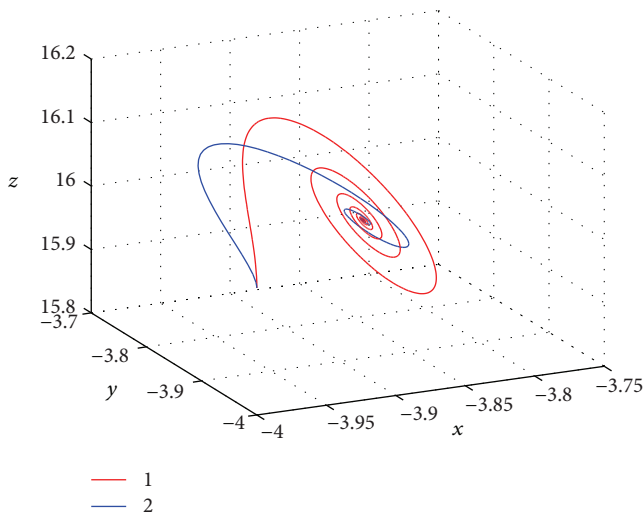FIGURE 20: Hopf bifurcation at E_+, when $c_1 = -5$, for case (iv).

FIGURE 21: Stable at E_- using controllers in [17] and this paper.

FIGURE 22: Stable at E_+ using controllers in [17] and this paper.

see that both controllers can stabilize the Lorenz system at equilibrium, and the controller designed in this paper is more simple and practical.

5. Conclusions

Aiming at the limitations of existing controller such as complex controller form, high order, including system equilibrium points in controller, and complicated solving method for parameters constraints, in this paper, a new parametric controller design method is proposed by researching and analyzing present Hopf bifurcation nonlinear system parametric controller design methods. This paper presents the design principle analysis and computation steps of this new parametric controller, designs a corresponding parametric controller for a Lorenz system example, deduces the constraints, and explains the controller method validity by numeric simulation. From simulation, compared with the other methods, it is easy to see that this new parametric controller method has simple form, lower order, not including any equilibrium point value.

Conflict of Interests

The authors declare that there is no conflict of interests regarding the publication of this paper.

Acknowledgment

References

[1] E. H. Abed and J.-H. Fu, "Local feedback stabilization and bifurcation control. I. Hopf bifurcation," *Systems & Control Letters*, vol. 7, no. 1, pp. 11–17, 1986.

[2] G. Chen and K. Yap, "Feedback control of Hopf bifurcations," *IEEE Transactions on Circuits and Systems I: Fundamental Theory and Applications*, vol. 6, pp. 661–672, 2001.

is the stable trajectory at E_-, and Figure 16 is the Hopf bifurcation trajectory at E_+. For case (iii), Figure 17 is the Hopf bifurcation trajectory at E_-, and Figure 18 is the stable trajectory at E_+. In accordance with condition (iv), Figure 19 is the Hopf bifurcation trajectory at E_-, and Figure 20 is the Hopf bifurcation trajectory at E_+.

Figures 21 and 22 are the system stable trajectories, using the controllers of this paper and [17]. Curve 1 is the system trajectory under the control of [17] and curve 2 is under the control of this paper. From Figures 21 and 22, it is easy to

[3] A. Jimenez-Triana, W. K.-S. Tang, G. Chen, and A. Gauthier, "Chaos control in duffing system using impulsive parametric perturbations," *IEEE Transactions on Circuits and Systems*, vol. 57, no. 4, pp. 305–309, 2010.

[4] C. Bi, Y. Xiang, Q. Zhang, and J. Hu, "Simulation study of bifurcation control in synchronous switching converter," in *Proceedings of the International Conference on Communications, Circuits and Systems (ICCCAS '13)*, vol. 2, pp. 463–466, Chengdu, China, November 2013.

[5] A. R. Phadke, M. Fozdar, K. R. Niazi, N. Mithulananthan, and R. C. Bansal, "New technique for computation of closest Hopf bifurcation point using real-coded genetic algorithm," *IET Generation, Transmission & Distribution*, vol. 5, no. 1, pp. 11–18, 2011.

[6] M. Tomim, B. Lopes, R. Leme et al., "Modified Hopf bifurcation index for power system stability assessment," *IEE Proceedings—Generation, Transmission and Distribution*, vol. 152, no. 6, pp. 906–912, 2005.

[7] A. Kavitha and G. Uma, "Experimental verification of Hopf bifurcation in DC–DC Luo converter," *IEEE Transactions on Power Electronics*, vol. 23, no. 6, pp. 2878–2883, 2008.

[8] F. Liu, H. O. Wang, and Z.-H. Guan, "Stability analysis and control of bifurcation in a TCP fluid flow model of wireless networks," in *Proceedings of the 10th World Congress on Intelligent Control and Automation (WCICA '12)*, pp. 1026–1030, IEEE, Beijing, China, July 2012.

[9] L. Yang, Z. Xu, J. Østergaard, Z. Y. Dong, K. P. Wong, and X. Ma, "Oscillatory stability and eigenvalue sensitivity analysis of a DFIG wind turbine system," *IEEE Transactions on Energy Conversion*, vol. 26, no. 1, pp. 328–339, 2011.

[10] K. E. Chlouverakis, K. M. Al-Aswad, I. D. Henning, and M. J. Adams, "Determining laser linewidth parameter from Hopf bifurcation minimum in lasers subject to optical injection," *Electronics Letters*, vol. 39, no. 16, pp. 1185–1187, 2003.

[11] M. Huang, C. K. Tse, S.-C. Wong, C. Wan, and X. Ruan, "Low-frequency hopf bifurcation and its effects on stability margin in three-phase PFC power supplies connected to non-ideal power grid," *IEEE Transactions on Circuits and Systems I: Regular Papers*, vol. 60, no. 12, pp. 3328–3340, 2013.

[12] P. S. Deivasundari, G. Uma, and R. Santhi, "Experimental verification of Hopf bifurcation in pulse-width modulated inverter fed cage induction motor drive system," *IET Power Electronics*, vol. 7, no. 2, pp. 340–349, 2014.

[13] N. G. Sakellaridis, M. E. Karystianos, and C. D. Vournas, "Homoclinic loop and degenerate hopf bifurcations introduced by load dynamics," *IEEE Transactions on Power Systems*, vol. 24, no. 4, pp. 1892–1893, 2009.

[14] G. Chen, J. L. Moiola, and H. O. Wang, "Bifurcation control: theories, methods, and applications," *International Journal of Bifurcation and Chaos*, vol. 10, no. 3, pp. 511–548, 2000.

[15] F. Liu, G. Xiong, Z.-H. Guan, and H. O. Wang, "Stability analysis and control Hopf bifurcation in a FAST TCP model," in *Proceedings of the 32nd Chinese Control Conference (CCC '13)*, pp. 1076–1080, Xi'an, China, July 2013.

[16] M. Xiao, W. X. Zheng, and J. Cao, "Hopf bifurcation of an (n + 1)-neuron bidirectional associative memory neural network model with delays," *IEEE Transactions on Neural Networks and Learning Systems*, vol. 24, no. 1, pp. 118–132, 2013.

[17] P. Yu and G. Chen, "Hopf bifurcation control using nonlinear feedback with polynomial functions," *International Journal of Bifurcation and Chaos in Applied Sciences and Engineering*, vol. 14, no. 5, pp. 1683–1704, 2004.

[18] T. Yang and X. Chen, "Local L_2 gain of Hopf bifurcation stabilization," in *Proceedings of the 47th IEEE Conference on Decision and Control (CDC '08)*, pp. 4103–4108, IEEE, Cancún, Mexico, December 2008.

[19] P. Cai, J.-S. Tang, and Z.-B. Li, "Controlling Hopf bifurcation of a new modified hyperchaotic Lü system," *Mathematical Problems in Engineering*, vol. 2015, Article ID 614135, 6 pages, 2015.

[20] F. Verduzco, J. Alvarez, and A. Carrillo, "Normal form and control of the Hopf bifurcation," in *Proceedings of the American Control Conference (ACC '07)*, pp. 2358–2363, New York, NY, USA, July 2007.

[21] Z. Wu and P. Yu, "A method for stability and bifurcation control," *IEEE Transactions on Automatic Control*, vol. 51, no. 6, pp. 1019–1023, 2006.

[22] Z.-Q. Wu, R. Ding, and Y.-S. Chen, "Classification of parametrically constrained bifurcations," *Applied Mathematics and Mechanics. English Edition*, vol. 31, no. 2, pp. 135–142, 2010.

[23] K. Cho and T. Miyano, "Chaotic cryptography using augmented lorenz equations aided by quantum key distribution," *IEEE Transactions on Circuits and Systems I: Regular Papers*, vol. 62, no. 2, pp. 478–487, 2015.

[24] R. Tokunaga, T. Matsumoto, L. O. Chua, and S. Miyama, "The piecewise-linear Lorenz circuit is chaotic in the sense of Shilnikov," *IEEE Transactions on Circuits and Systems*, vol. 37, no. 6, pp. 766–786, 1990.

[25] S. Yu, J. Lu, X. Yu, and G. Chen, "Design and implementation of grid multiwing hyperchaotic Lorenz system family via switching control and constructing super-heteroclinic loops," *IEEE Transactions on Circuits and Systems*, vol. 59, no. 5, pp. 1015–1028, 2012.

[26] A. Dwivedi, A. K. Mittal, and S. Dwivedi, "Adaptive synchronisation of diffusionless Lorenz systems and secure communication of digital signals by parameter modulation," *IET Communications*, vol. 6, no. 13, pp. 2016–2026, 2012.